Electroabsorption study of excited states in tris 8-hydroxyquinoline aluminum complex

ARTICLE *in* CHEMICAL PHYSICS LETTERS · FEBRUARY 1998

Impact Factor: 1.9 · DOI: 10.1016/S0009-2614(97)01343-2

13 February 1998

ELSEVIER

Chemical Physics Letters 283 (1998) 373–380

CHEMICAL PHYSICS LETTERS

Electroabsorption study of excited states in tris 8-hydroxyquinoline aluminum complex

W. Stampor [a], J. Kalinowski [a,b], G. Marconi [b], P. Di Marco [b], V. Fattori [b], G. Giro [b]

[a] *Department of Molecular Physics, Technical University of Gdańsk, ul. Narutowicza 11 / 12, 80-952 Gdańsk, Poland*
[b] *Istituto di Fotochimica e Radiazioni di Alta Energia (FRAE) del C.N.R., Via P. Gobetti 101, 40129 Bologna, Italy*

Received 19 August 1997; in final form 21 November 1997

Abstract

Electric field-modulated absorption spectra, from 280–490 nm, of vacuum-evaporated films of tris (8-hydroxyquinoline) aluminum (Alq_3) have been studied to determine the polarity of the electronic excited states. Semiempirical molecular modelling has been employed to relate the energetics and molecular electrical dipole moments of the isolated molecule to those resulting from the electroabsorption experiment, interpreted in terms of the second-order Stark effect. The results indicate the lowest excited singlets with relatively small dipole moments to be well localized on individual quinolate ligands, and those with higher energy and large dipole moments to show delocalization by charge transfer to the nearest-neighbour ligands of different molecules. The implications for the electroluminescent behaviour of Alq_3 are discussed. © 1998 Elsevier Science B.V.

1. Introduction

The aluminum (III) 8-hydroxyquinoline complex (Alq_3) is one of the most common vacuum-deposited organic light emitters in the newest class of organic heterojunction devices — organic light-emitting-diodes (LEDs) [1,2]. Since one of the major factors that determines electroluminescence (EL) efficiency is the decay mechanism of excited states, there has been considerable interest in the optical properties of this complex as well as other metal 8-hydroxyquinoline chelates (Mq_3) [2–7]. A large Stokes shift (0.4–0.7 eV) between the broad emission and first absorption transition in Alq_3 which was first ascribed to excimers [8] seems to be more probably associated with large local conformational changes, as comes from a theoretical analysis of its molecular structure [2]. It has been suggested that the electronic $\pi-\pi^*$ transitions in Alq_3 are localized on the quinolate ligands; the three lowest electronic transitions being donor–acceptor transitions from a phenoxide donor to a pyridyl acceptor side of the quinolate ligands [2]. The structural distortion of the molecule following these transitions leads to deep energy localization of the first excited singlet. For the same reasons an excessive electron (e.g. injected from an electrode contact) is expected to localize on the pyridyl side of the quinolate ligands. These suppositions provide insight into the nature of the excited states in Alq_3 in the absence of an electric field. In organic LEDs the emissive layer is subjected to electric fields (F) often exceeding 10^6 V/cm, therefore one would expect some modifications of excited states. For instance, intermolecular charge transfer transitions

PII S0009-2614(97)01343-2

can be alleviated by such a high electric field, resulting in formation of separated electron-hole pairs. Consequently, a drop in the number of emitting states is expected. In fact, as much as a 60% decrease in the population of excited singlets has been predicted in thin films of Alq_3 at fields exceeding 10^6 V/cm, based on field-induced luminescence quenching experiments [7]. Moreover, electric field-induced energy level shifts (ΔE) due to electrical moment changes ($\Delta\mu$) can be of importance. For example, $\Delta E = -\Delta\mu\, F \cong \pm 0.1$ eV for $\Delta\mu = \pm 20$ D and $F = 3 \times 10^6$ V/cm.

To gain insight into the electric field effect on the excitation process of electronic states and its possible role in organic EL devices, we studied the electroabsorption (EA) spectra of solid films of Alq_3 sandwiched between two semitransparent aluminum electrodes, applying fields of up to $\approx 10^6$ V/cm. The results are discussed within the framework of the second-order Stark effect. The experimental data are in good agreement with the theoretical predictions related to the energetics and electric dipole moments of the molecular excited states as calculated using a semi-empirical approach, ZINDO/S [9], and taking into account the crystal structure of Alq_3 [10].

2. Sample preparation and experimental procedure

The measurements were performed on a $d = 550$ nm thick film of Alq_3 evaporated onto a semitransparent layer of oxidized aluminum on room-temperature quartz substrate and then covered by another semitransparent layer of Al using a conventional vacuum deposition technique. Prior to its use, commercially available Alq_3 was purified by sublimation and stored in the dark. The experimental apparatus, used to record the electric field-induced change in the light intensity passing through the cell as a function of the wavelength, allowed illumination in the applied field direction. The light sources used were a halogen lamp (Polam 250 W) and a mercury lamp (Narva 200 W) followed by a SPM-2 Zeiss

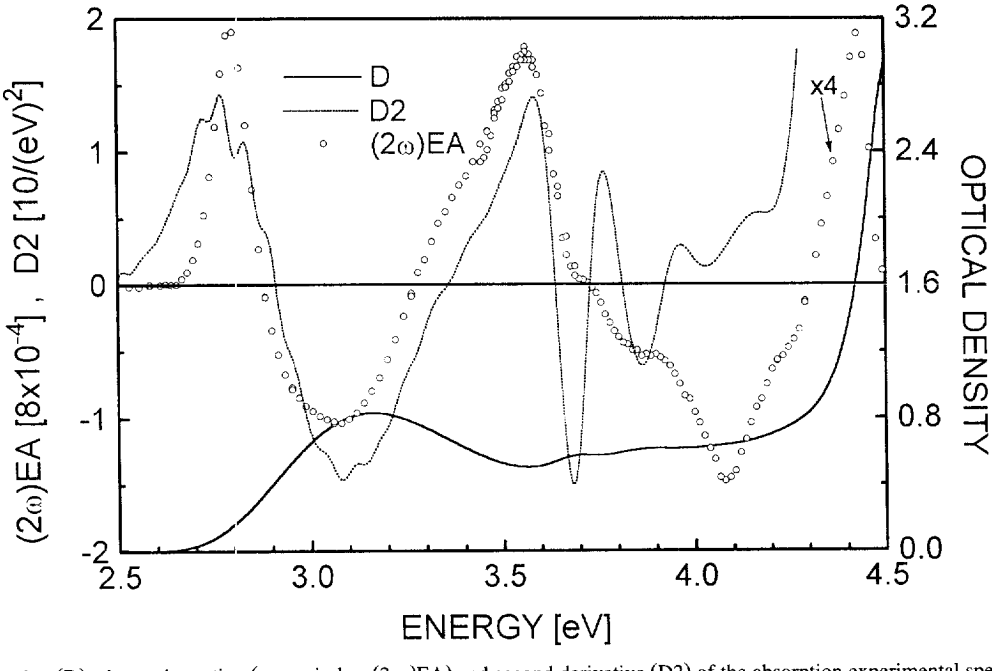

Fig. 1. Absorption (D), electroabsorption (open circles; (2 ω)EA) and second derivative (D2) of the absorption experimental spectra obtained on a 550 nm thick Alq_3 film, prepared by a vacuum evaporation technique. The field amplitude for the EA spectrum $F_m = 9.3 \times 10^5$ V/cm.

monochromator. Electromodulation of the absorption was induced by a sinusoidal electric field ($\omega/2\pi =$ 175 Hz) between 0.05 MV/cm and 1 MV/cm. The EA signal was recorded at the second harmonic employing phase-sensitive techniques. Field-induced changes in the transmitted intensity ($\Delta I/I = -\Delta\alpha\, d$, where d is the sample thickness and $\Delta\alpha$ is the field-induced change in the absorption coefficient of the sample) of less than 10^{-5} could be resolved with a spectral resolution of about 100 cm^{-1}. The EA signals increased with the square of the applied voltage independent of the wavelength (cf. Fig. 2 of Ref. [7]). All spectra were monitored at constant optical resolution.

3. Results and discussion

Fig. 1 shows the room temperature ordinary absorption (D) and electroabsorption (EA) spectra of the Alq_3 film described in Section 2. The absorption spectrum consists of a low-energy broad band at about 3.15 eV, a quasi-flat segment between 3.6 and 4.2 eV and a strongly increasing wing towards 4.5 eV. The weak features in the second region are much better resolved in the second derivative (D2) of the absorption spectrum. The D2 spectrum has been obtained from the numerical data of the absorption curve using well-known methods including suitable smoothing procedures. A direct comparison reveals that the second harmonic (2ω)EA spectrum fits the second derivative within the first absorption band well and differs substantially above 3.8 eV.

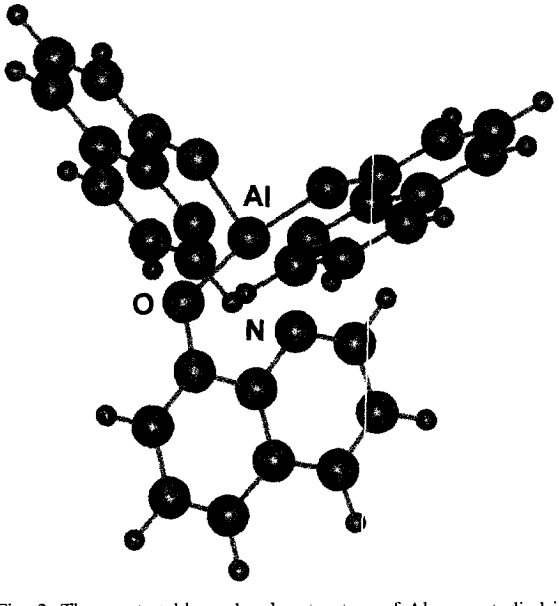

Fig. 2. The most stable molecular structure of Alq_3 as studied in detail with ZINDO/S in the present Letter.

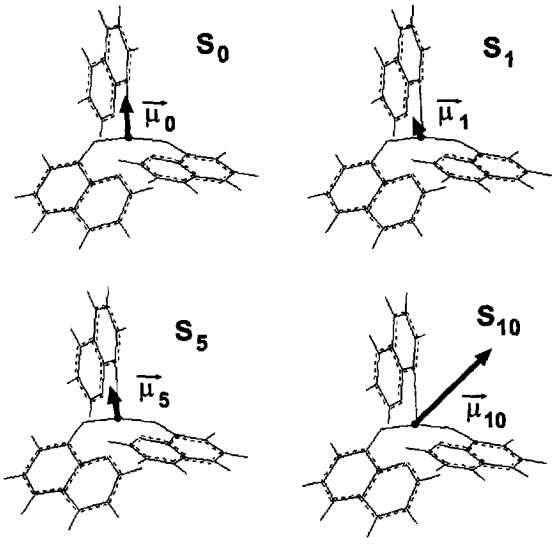

Fig. 3. Selected permanent dipole moments (μ_n) of isolated molecules of Alq_3 in the ground (S_0) and three different singlet excited states (S_1, S_5, S_{10}). The zero of the coordinate reference system is located on the Al atom. The values of μ_n are expressed in Ångström (for Debye units see Table 1).

The root-mean-square values of the EA signal can be expressed as [11]

$$\left(\frac{\Delta I}{I}\right)_{2\omega} = \frac{\ln 10}{2\sqrt{2}} F^2_{\mathrm{m.loc.}} \times \sum_n \left[\frac{1}{2}\bar{\Delta} p_n \frac{\mathrm{d}D_n}{\mathrm{d}E} + \frac{1}{6}(\Delta m_n)^2 \frac{\mathrm{d}^2 D_n}{\mathrm{d}E^2}\right] = \sum_n \left(a_n \frac{\mathrm{d}D_n}{\mathrm{d}E} + b_n \frac{\mathrm{d}^2 D_n}{\mathrm{d}E^2}\right) \quad (1)$$

with $a_n = (\ln 10/4\sqrt{2}) F^2_{\mathrm{m.loc.}} \cdot \bar{\Delta} p_n$ and $b_n = (\ln 10/12\sqrt{2}) F^2_{\mathrm{m.loc.}} (\Delta m_n)^2$ where $\bar{\Delta} p_n$ and Δm_n are the spatially averaged polarizability and dipole moment change on the nth electronic transition, respectively, and D_n is the optical density of the nth transition, differentiated in Eq. (1) by the energy E.

$F_{m.loc.}$ corresponds to the external field amplitude which can be estimated as $F_{m.lcc.} = (\varepsilon + 2)U_m/3d$ in the Lorentz approximation model for the local field. It is assumed that the external field is homogeneous within the sample of dielectric constant ε and of thickness d with the applied voltage $U = U_m \sin(\omega t)$.

The (2ω)EA spectrum in the range 2.6–3.7 eV can be fitted well with a simplified version of Eq. (1), neglecting the contribution of the first derivative term, i.e.

$$\left(\frac{\Delta I}{I}\right)_{2\omega} \cong b\frac{d^2D}{dE^2}. \quad (2)$$

The fitting procedure with the value $\varepsilon = 3.8$ measured by us, using the Lorentz field approximation, yields the average $\Delta m \cong 6.3$ D. This implies that in the long-wavelength region (< 3.6 eV), the EA signal follows the second derivative of the first broad absorption band well, the effect being determined by electric-field-induced broadening of the energy levels of the states differing in their dipole moments by about 6.3 D.

For a more exact interpretation, molecular orbital calculations have been carried out for the isolated Alq_3 molecule. Starting from the X-ray geometry [10], a molecular mechanics (MM^+) calculation [12] has been performed for a search of the most stable ground-state geometry. In agreement with the results of previous calculations [13], the most stable isomer found was that with a "meridianal" conformation (see Fig. 2). The optimized geometry was then used to calculate the excited states of the molecule using the ZINDO/S Hamiltonian [9], within a space of 144 singly excited configurations. The resulting lowest excited singlets, deriving from HOMO → LUMO transitions and corresponding to the first absorption range, show mostly lower dipole moments with respect to the ground state, a feature that seems in agreement with their delocalized, donor–acceptor, character (see Fig. 3). The calculated first 17 molecular singlet state energies and corresponding dipole moments are summarized in Table 1. The values of the dipole moments of some higher singlet states such as for example S_{10}, S_{11} or S_{13}, are large, exceeding that of the ground state which has been found to be $m_G = 7.77$ D. A singlet exciton can be readily quenched by a trapped (or free) charge injected into the emitter layer forming a part of an

Table 1
Spectral features of Alq_3

Molecular state (S_n)	E_n' (eV)	f_n	m_n (D)	Δm_n (D)[a]	A_r (f_n/f_1)	EA_r (I_n/I_1)[b]	$E_n = E_n' - \Delta E$ (eV)
S_1	3.48	0.193	4.9	9.4	1.000	1.00	3.08
S_2	3.59	0.178	5.4	4.5	0.922	0.21	3.19
S_3	3.67	0.075	8.4	4.7	0.389	0.10	3.27
S_4	4.15	0.0009	14.3	17.0	0.005	0.02	3.75
S_5	4.181	0.024	4.0	4.7	0.124	0.03	3.781
S_6	4.184	0.020	4.4	6.1	0.104	0.04	3.784
S_7	4.21	0.010	8.2	3.2	0.052	0.01	3.81
S_8	4.33	0.0005	18.8	25.2	0.003	0.02	3.93
S_9	4.45	0.0002	20.7	24.2	0.001	0.01	4.05
S_{10}	4.57	0.0009	26.7	22.8	0.005	0.03	4.17
S_{11}	4.59	0.007	24.9	21.0	0.036	0.18	4.19
S_{12}	4.636	0.0007	3.8	12.0	0.004	0.01	4.236
S_{13}	4.64	0.004	23.3	22.8	0.005	0.12	4.24
S_{14}	4.82	0.0004	14.3	11.5	0.002	0.003	4.42
S_{15}	4.99	0.002	16.1	18.6	0.010	0.04	4.59
S_{16}	5.13	0.073	6.6	1.7	0.378	0.01	4.73
S_{17}	5.19	0.744	4.6	4.1	3.855	0.74	4.79

E_n' = predicted singlet state energies; f_r = oscillator strengths; m_n = absolute electrical dipole moments; Δm_n = dipole moment change upon excitation; A_r = relative absorption and EA_r = relative electroabsorption for isolated molecule; E_n = experimentally assigned excited singlet energies in solid state films.

[a] $\Delta m_n = |\vec{m}_n - \vec{m}_G|$, where $m_G = 7.77$ D is the dipole moment of the isolated molecule in the ground state.

[b] $I_n = f_n(\Delta m_n)^2$.

organic LED. The exciton–charge carrier annihilation rate is determined by both their relative motion and the elementary capture process at the reaction site (localized exciton or charge carrier). The capture is by definition dependent on the exciton–charge carrier interaction potential. If, as in the case of anthracene singlet exciton quenching by tetracene molecules dopant, the rate is capture limited [14], the dipole moment of the excited state is expected to influence the overall quenching constant since it enters the interaction part of the Hamiltonian. The dipole moment altered channel for exciton decay by its interaction with charge carriers is relevant to the EL efficiency of organic LEDs [15] and should not be lost from the field of vision. Table 1 also lists the predicted oscillator strengths and experimentally assigned excited state energies. From the comparison between the theoretical predictions of the molecular singlet state energies (Table 1) and those obtained by decomposition of the experimental absorption spectrum into five individual transition bands, one can note a 0.4 eV red shift for the experimentally observed transitions (see Fig. 4). This is the gas to crystal energy shift arising from a non-resonance interaction between an excited molecule and its surrounding medium. In a periodic lattice it has a discrete value. Assuming the intermolecular distances and polarizability of the crystal matrix to be independent of the molecular excitation level, $\Delta E = 0.4$ eV should be roughly conserved for all electronic transitions. Thus, the energies of excited singlets above S_5 in solid Alq_3 can be predicted using their theoretical values for isolated molecules (see the last column of Table 1). Due to the low value of the oscillator strength for the S_4 state, a substantial absorption in the energy range under study (2.5–4.5 eV) should belong to transitions S_1, S_2, S_3 and S_5, S_6. Indeed, the experimental absorption spectrum can be reproduced by the superposition of five Gaussian components with the first maximum absorption at ≈ 392 nm (3.16 eV) (see Fig. 4).

In contrast, strong EA structures appear at energies (≈ 3.6 eV, ≈ 4.1 eV) which correspond to the weak transitions S_4 and S_{10}, S_{11}, S_{12} and S_{13}.The

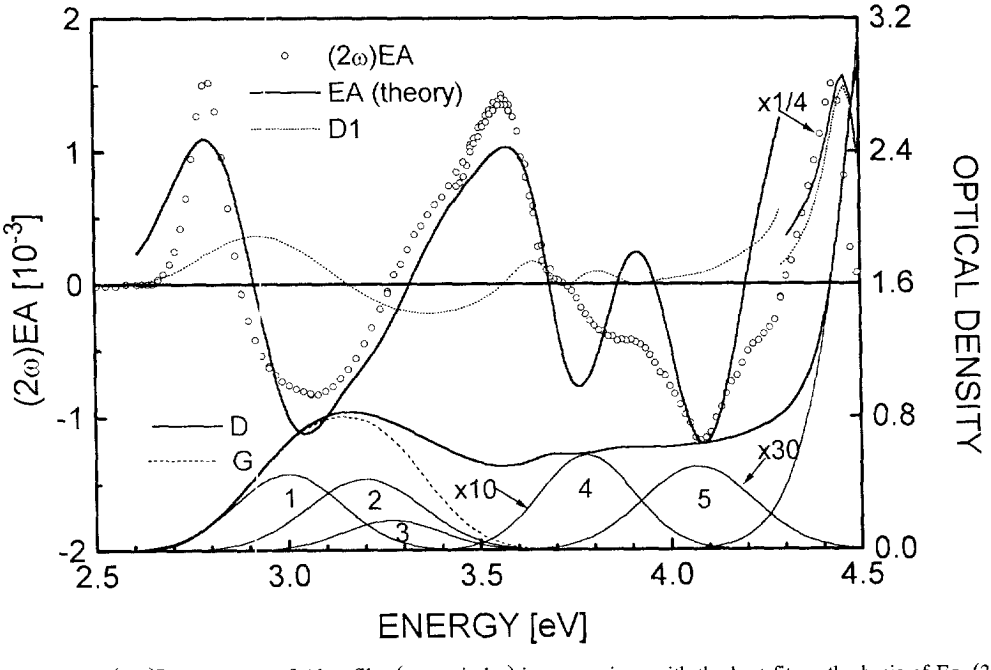

Fig. 4. The experimental (2ω)EA spectrum of Alq_3 film (open circles) in comparison with the best fit on the basis of Eq. (3) (solid line) and with the contribution to the EA spectrum of the first derivative of the absorption spectrum D1 (dotted line). The experimental absorption spectrum (D) and its profile analysis is displayed in the lower part of the figure. The dashed line shows the absorption band composed of the first three Gaussian components of the D spectrum.

reason for this behaviour may be understood by noting that the EA intensity, I_n, is governed by a product of the oscillator strength and square of the dipole moment change upon the transition between the ground and excited states ($I_n = f_n\,(\Delta m_n)^2$, $\Delta m_n = |m_n - m_G|$). Application of the formula for I_n containing the oscillator strength and the change in the electrical dipole moment upon excitation gives EA intensity for each of the 17 transitions listed in Table 1 (7th column denoted $EA_r \equiv$ relative EA intensity). The most striking is the strong EA signal for S_{11} which, due to the small $f_{11} = 0.007$, does not appear in the ordinary absorption but because of the high polarity ($m_{11} = 24.9$ D; see dipole moments for other excited states given for comparison in Fig. 3) shows up as a strong EA feature confirmed by the experimental data of Fig. 4. The shape of the theoretical EA spectrum presented in this figure is a result of superposition of the first derivative of the absorption spectrum ($D1 = dD/dE$) and of the second derivatives of five Gaussian bands, corresponding to the singlet states resolved from the experimental absorption spectrum:

$$\left(\frac{\Delta I}{I}\right)_{2\omega} = a\frac{dD}{dE} + \sum_{n=1}^{5} b_n \frac{d^2 D_n}{dE^2}. \qquad (3)$$

The first derivative contribution has been weighted by the average polarizability change Δp between the ground and excited states. With the Lorentz approximation for the local electric field, the present fit of the spectrum yields $\Delta p \cong 16$ Å^3. This is an order of magnitude characteristic of Frenkel excitons in solid films of some other polar compounds as for instance $\Delta p \cong 36$ Å^3 in thionapthenoindole [16]. The difference can be associated with the presence of stronger intermolecular charge transfer (CT) states which seemed to cause a reduction of Δp in solid films of a non-polar compound (linear trans-quinacridone) [11]. Possible variations in the internal electric field strengths found to operate in illuminated thin organic films [17] do not influence the second harmonic EA signal [16].

The fitting procedure involving Eq. (3) allowed the coefficients b_n to be determined and then Δm_n(exp) to be compared with Δm_n(theor) as given in Table 1. To avoid an inaccuracy in evaluating absorption intensities from the decomposition of the absorption spectrum into Gaussian components (which is not unique), we have used the oscillator strengths predicted for these transitions in the isolated molecules. The results are displayed in Table 2. An apparent difference between values of Δm_n(exp) and Δm_n(theor) suggests additional dipole moments appearing upon optical excitation. We speculate that Δm_n (exp) represents a sum of the molecular permanent dipole moment change $\Delta \mu_n$, and a dipole moment, Δm_n (CT), appearing as a result of the intermolecular charge transfer (CT) transition upon excitation: $\Delta m_n = \Delta \mu_n + \Delta m_n$ (CT). The values of Δm_n (CT) for eight transitions of interest are shown in the 8th column of Table 2. They correspond to one electron transfer over a distance < 1 Å for the

Table 2
Results of the band resolution of the second derivative contribution of the EA spectrum, of Alq_3 with energies predicted from ZINDO/S calculations and red shifted by 0.4 eV (theor) and those obtained from the decomposition of the experimental spectrum into Gaussian component (exp). Intensiteis used in the fitting procedure according to Eq. (3) were taken from Table 1 for the electronic transitions on isolated molecules

Absorption band	Assignment	Energy (theor.) (eV)	Energy (exp.) (eV)	Width (exp.) (eV)	Δm_n(theor.) (D)	Δm_n(exp.) (D)	Δm_n(CT) (D)[a]
1	2	3	4	5	6	7	8
1	S_1	3.08	3.00	0.33	9.4	5.8	−3.6
2	S_2	3.19	3.19	0.35	4.5	5.1	0.6
3	S_3	3.27	3.27	0.30	4.7	–	–
4	S_5	3.781	3.78	0.29	4.7	14	9.3
	S_6	3.784			6.1	33	7.9
5	S_{10}	4.17	4.07	0.35	22.8		10.2
	S_{11}	4.19			21.0		12
	S_{13}	4.24			22.8		10.2

[a] $\Delta m_n(CT) = \Delta m_n(exp.) - \Delta \mu_n$, where $\Delta \mu_n = \Delta m_n(theor.)$.

lowest localized states S_1–S_3, through ≈ 2 Å for the states S_5 and S_6 and up to ≈ 3 Å for the highest energy states S_{10}–S_{13}. The latter is close to the electron hopping distances 3.9 Å, 4.9 Å obtained from the luminescence quenching experiments [7], assuming the charge separation process is competing with radiative decay of the excited states. It is interesting to note that the interplanar distance between quinolate ligands of the two closest located molecules of the four molecules constituting the elementary cell of the Alq_3 crystal is ≈ 2.5 Å [10]. This would suggest that except for the lowest excited states (S_1–S_3) which are well localized on one quinolate ligand, the higher energy states are a mixture of the local Frenkel and intermolecular CT state created by the electronic charge displacement between two quinolate ligands. Moreover, since the above distance between the quinolate pairs lies within the range of an attractive excimer interaction for planar molecules like pyrene [18], formation of the excimer-type species between such pairs cannot be excluded in Alq_3. The question arises how it can be reconciled with the glassy nature of vacuum-deposited Alq_3 films considered as a solid solution of the meridianal and facial isomers of this compound [2]. The present results suggest that solid Alq_3 films represent an example for molecular solids with a degree of disorder intermediate between that of a completely random system (strong disorder) and of a system exhibiting long-range order typical for single crystals. They are characterized by the presence of molecular aggregates whose structure is similar to the crystal structure. Statistical fluctuations of the molecular coordinates, the degree of which they depend on the formation conditions of solid, cause a splitting of the exciton bands into a distribution of localized states and the absorption profile maps the energy distribution of the absorbing sites. It reflects directly the degree of frozen-in disorder. The intermediate structural disorder has been observed in solid films of aromatic hydrocarbons such as tetracene and pentacene [19].

4. Concluding remarks

Measurements of the absorption and electroabsorption spectra of solid films of Alq_3 allow the extraction of quantitative information concerning charge distribution around the excited sites due to optical electronic transitions. They demonstrate that for the lowest excited singlets (S_1–S_3), the charge is localized on individual quinolate ligands (as has been already pointed out by other authors [2]), but shows delocalization to the nearest-neighbour ligands of different molecules in the crystalline structure for high energy transitions (S_5 and above). The results are in good agreement with the prediction of theoretical calculations based upon molecular mechanics, semi-empirical modelling of electronic states ZINDO/S and the second-order Stark effect. The present work substantiates the intuitive conclusion that the crystalline molecular environment should influence the properties of excited states, the isolated molecule excited states being only a reference frame for their counterparts in the solid state. The charge distribution on individual ligands leading to the relatively high molecular electrical dipole moment in the ground state undergoes meaningful evolution upon excitation, with an appropriate change of dipole moments. Whereas a strong polarity of ligand-localized excited states makes their possible annihilation with charge carriers more efficient, the intermolecular ligand charge transfer leads directly to exciton quenching by creation of separated electron–hole pairs. Both should be taken into account in operation mechanisms of organic LEDs.

References

[1] J. Kalinowski, Organic Electroluminescent Materials and Devices, in: S. Miyata, H.S. Nalwa (Eds.), Gordon and Breach, Amsterdam, 1997, chap. 1.
[2] S.R. Forrest, P.E. Burrows, M.E. Thompson, Organic Electroluminescent Materials and Devices, in: S. Miyata, H.S. Nalwa (Eds.), Gordon and Breach, Amsterdam, 1997, chap. 13.
[3] R. Ballardini, G. Varani, M.T. Indelli, F. Scandola, Inorg. Chem. 25 (1986) 3858.
[4] D.Z. Garbuzov, V. Bulovic, P.E. Burrows, S.R. Forrest, Chem. Phys. Lett. 249 (1996) 433.
[5] A.D. Walser, I. Sokolik, R. Priestley, R. Dorsinville, Appl. Phys. Lett. 69 (1996) 1677.
[6] I. Sokolik, R. Priestley, A.D. Walser, R. Dorsinville, C.W. Tang, Appl. Phys. Lett. 69 (1996) 4168.
[7] W. Stampor, J. Kalinowski, P. Di Marco, V. Fattori, Appl. Phys. Lett. 70 (1997) 1935.

[8] J. Kalinowski, N. Camaioni, P. Di Marco, V. Fattori, G. Giro, Int. J. Electronics 81 (1996) 377.
[9] A.D. Bacon, M.C. Zerner, Theor. Chim. Acta 53 (1979) 21.
[10] H. Schmidbaur, J. Lettenbauer, D.L. Wilkinson, G. Mueller, O. Kumberger, Z. Naturforsch. 46 b (1991) 901.
[11] J. Kalinowski, W. Stampor, P. Di Marco, V. Fattori, Chem. Phys. 182 (1994) 341.
[12] N.L. Allinger, J. Am. Chem. Soc. 99 (1977) 8127.
[13] P.E. Burrows, Z. Shen, V. Bulovic, D.M. McCarty, S.R. Forrest, J.A. Cronin, M.E. Thompson, J. Appl. Phys. 79 (1996) 7991.
[14] D. Schmid, Organic Molecular Aggregates, in: P. Reineker, H. Haken, H.C. Wolf (Eds.), Springer, Berlin, 1983, p. 184.
[15] J. Kalinowski, Polymers and Other Advanced Materials: Emerging Technologies and Business Opportunities, in: P.N. Prasad, E. Mark, J.F. Fung (Eds.), Plenum, New York, 1995, p. 361.
[16] W. Stampor, J. Kalinowski, P. Di Marco, Chem. Phys. 134 (1989) 385.
[17] W. Stampor, J. Kalinowski, P. Di Marco, Mol. Cryst. Liq. Cryst. 228 (1993) 233.
[18] M. Pope, C.E. Swenberg, Electronic Processes in Organic Crystals, Clarendon, Oxford, 1982, p. 50.
[19] R. Hesse, W. Hofberger, H. Bässler, Chem. Phys. 49 (1980) 201.